Cells & Development xxx (xxxx) xxx

Contents lists available at ScienceDirect

Cells & Development

journal homepage: www.journals.elsevier.com/cells-and-development

Tissue mechanics modulate morphogen signalling to induce the head organiser

Matyas Bubna-Litic [a], Guillaume Charras [a,b], Roberto Mayor [a,c,*]

[a] Department of Cell and Developmental Biology, University College London, Gower Street, London WC1E 6BT, UK
[b] London Centre for Nanotechnology, University College London, Gordon St, London WC1H 0AH, UK
[c] Center for Integrative Biology, Faculty of Sciences, Universidad Mayor, Santiago, Chile

ARTICLE INFO

Keywords:
Embryonic induction
Mesoderm
Tissue mechanics
Head organiser
Morphogenesis
Self-organization

ABSTRACT

Morphogenetic movements and specification of germ layers during gastrulation are key processes that establish the vertebrate body plan. Despite substantial research into the role of tissue mechanics during gastrulation and detailed characterisation of the molecular signalling networks controlling fate determination, the interplay of mechanical cues and biochemical signals during fate specification is poorly understood. Morphogens that activate Activin/Nodal/Smad2 signalling play a key role in mesoderm induction and axial patterning. We investigate the interplay between a single molecular input and a mechanical input using the well-established *ex vivo* system of Activin-induced explants of the mid-blastula *X. laevis* animal cap ectoderm. Activin alone induces mesoderm to form a complex elongating tissue with axial patterning, making this system similar to gastruloids generated in other model organisms. We observed an increase in the expression of dorsal mesoderm markers, such as *chordin* and *goosecoid*, and loss of elongation, in Activin-induced explants that were mechanically stimulated through uniaxial compression during the induction period. In addition, head mesoderm specific markers, including *cerberus 1*, were also increased. We show that mechanical stimulation leads to an increase in nuclear β-catenin activity. Activation of β-catenin signalling is sufficient to induce head Organiser gene expression. Furthermore, inhibition of β-catenin is sufficient to rescue the effect of compression on an early Wnt-signalling response gene *siamois*. Taken together these observations support the role of mechanical stimulation in modulating Activin-dependent mesoderm induction in favour of head Organiser formation. Given the conserved role of β-catenin in the dorsal specification and the dynamic morphogenetic movements of dorsal gastrula regions, mechanics-dependent Organiser induction may be found in other vertebrate species. Finally, the finding that mechanical cues affect β-catenin-dependent axial specification can be applied in the future development of more biologically relevant and robust synthetic organoid systems.

1. Introduction

This article is a contribution to the Special Issue of *Cells & Development*, celebrating one hundred years since the most famous experiment in embryology, where Hans Spemann and Hilde Mangold discovered that transplanting the dorsal blastopore lip of an amphibian gastrula to the ventral side of a host embryo induced the formation of a secondary embryonic axis (Spemann and Mangold, 1924). This seminal discovery laid the foundation for research on embryonic induction. Today, it is widely accepted that vertebrate development depends on embryonic induction events, where one cell population influences the fate and morphogenetic processes of another (Niehrs, 2004; Joubin and Stern, 2001). In early embryogenesis, induction allows for establishing primary body axes and separating germ layers (Kiecker et al., 2016; Agius et al., 2000). Information transfer between different populations is primarily driven by a combination of two types of interactions: *molecular signalling* through diffusible ligands or receptor-receptor interactions, and *physical interactions* such as tissue deformation or geometric constraints (Vianello and Lutolf, 2019; Collinet and Lecuit, 2021). The experiments by Spemann and Mangold were among the first to demonstrate embryonic induction through the discovery of the amphibian Organiser (Spemann and Mangold, 1924; Niehrs, 2004). It was not until the successes of developmental genetics and molecular biology in the late 1980s that a mechanism that regulates induction of

* Corresponding author at: Department of Cell and Developmental Biology, University College London, Gower Street, London WC1E 6BT, UK.
E-mail address: r.mayor@ucl.ac.uk (R. Mayor).

https://doi.org/10.1016/j.cdev.2024.203984
Received 10 October 2024; Received in revised form 26 November 2024; Accepted 29 November 2024
Available online 2 December 2024

the mesoderm and establishment of the Spemann-Mangold Organiser was described in *X. laevis* (Kiecker et al., 2016; Dale and Slack, 1987; Dale, 1997). The concept of organising centres has been extended to other animal model organisms, including chicken (Joubin and Stern, 1999), zebrafish (Agathon et al., 2003), mouse (Knoetgen et al., 2000) and hydra (Reddy et al., 2019). The accepted view today is that the regulative control of early embryonic induction relies on the action of morphogen molecules that specify different fates along opposing gradients (Gurdon and Bourillot, 2001; Crease et al., 1998).

More recent work in chick (Saadaoui et al., 2020), zebrafish (Brunet et al., 2013), and human embryonic stem cells (Muncie et al., 2020) has highlighted the integral and conserved role mechanotransduction plays in early germ layer formation (De Belly et al., 2022; Piccolo et al., 2022; Miller and Davidson, 2013). Here we consider the role of tissue mechanics in the process of mesoderm induction in early development. Forces produced by morphogenetic events including epiboly, blastocoel expansion (Alasaadi et al., 2024) as well as convergence and extension (Chien et al., 2015; Shook et al., 2018; Papan et al., 2007) are a likely source of mechanical cues in pre-gastrula *X. laevis* embryos during the time of mesoderm and Organiser formation. We hypothesised that mechanotransduction modulates biochemical morphogen signalling and therefore contributes to early fate determination. To address this central question of the interplay between a morphogen signal and mechanical cues, we used an *ex vivo* system where the signal intensity and duration can be varied experimentally.

The established *ex vivo* model of mesoderm induction in *X. laevis* by treatment of mid-blastula (onset of Stage 9) derived animal cap explants with the morphogen Activin (Ninomiya et al., 2004; Green et al., 2004) is a suitable system to investigate the interplay between biochemical and mechanical signals (Fig. 1A). Animal cap induction is an early example of a gastruloid, a type of *in vitro* embryo model system that recapitulates aspects of *in vivo* gastrulation, and its use has recently been reviewed (Moris et al., 2020; Emig and Williams, 2023). Activin treatment enables dosage and temporal control, unlike the potentially original gastruloid system developed by Johannes Holtfreter in 1943 by isolating the dorsal lip of the blastopore which relies on endogenous mesoderm inducing signals (Holtfreter, 1943).

The animal cap explant is composed of a superficial epithelial layer and a deep layer that exhibits dynamic cell interactions and rearrangements (Green and Smith, 1990). The 2–3 cell layers thick deep layer contains pluripotent presumptive ectoderm that is receptive to the mesoderm inducing activity of Activin (Ariizumi et al., 2017). Note that *in vivo* this tissue is separated from mesoderm inducing signals by the blastocoel cavity allowing for the treatment with individual molecular inputs in isolated explants (Dale, 1997). For this reason, the animal cap induction assay has been instrumental in the identification of molecular inducers of mesoderm and neuroectoderm (Crease et al., 1998; Green and Smith, 1990; Green et al., 1997; Cornell and Kimelman, 1994). Remarkably, induced animal cap explants can develop into many tissue types including kidney, cardiac and skeletal muscle and the notochord when exposed to the different combinations of molecular inducers (Ariizumi et al., 2017; Uochi and Asashima, 1996; Logan and Mohun, 1993). The formation of different types of mesoderm along the primary embryonic axes and the ability to exhibit elongation through self-organised convergence and extension means that the induced animal cap is an accessible and versatile gastruloid system (Ninomiya et al., 2004; Green et al., 2004).

By combining the Activin-dependent induction assay with mechanical stimulation we have investigated the interplay between chemical and mechanical cues in the context of early mesoderm induction. This approach allowed us to induce mesodermal fate specification using a single morphogen signal *ex vivo* and avoid confounding effects from other signalling molecules or sources of mechanical stimulation present *in vivo*. Furthermore, this set up allowed for the mechanical deformation of the induced tissue without displacement of signal producing and receiving tissues that arise from physical manipulations *in vivo*. We observed that uniaxial compression of explant tissue during Activin treatment leads to the activation of gene expression characteristic of the anterior (head) region of the Organiser. Furthermore, we examined the role of β-catenin in the modulation of Activin signalling through mechanical compression. Taken together, these results imply a role for mechanical cues in the formation of a crucial signalling centre.

2. Results

2.1. Morphogen induction of animal cap explant gastruloids

Animal cap explants were used in combination with mechanical stimulation to investigate the interplay between biochemical and mechanical cues during fate specification. Without additional signals, animal cap explants cultured *in vitro* in a neutral medium become spherical and form ectoderm-derived epithelium (Fig. 1B). Animal cap explants taken at competent blastula stages can be induced with Activin to express mesodermal markers in a dose and time dependent manner (Green and Smith, 1990; Ariizumi et al., 1991; Bright et al., 2021). At medium doses of Activin (1–10 ng/mL) induced explants express mesodermal markers including *tbxt* (commonly known as *brachyury*) and *gsc* and give rise to skeletal muscle expressing *actc1* (Fig. 1C) (Green et al., 1997; Ariizumi et al., 1991; Satou-Kobayashi et al., 2021).

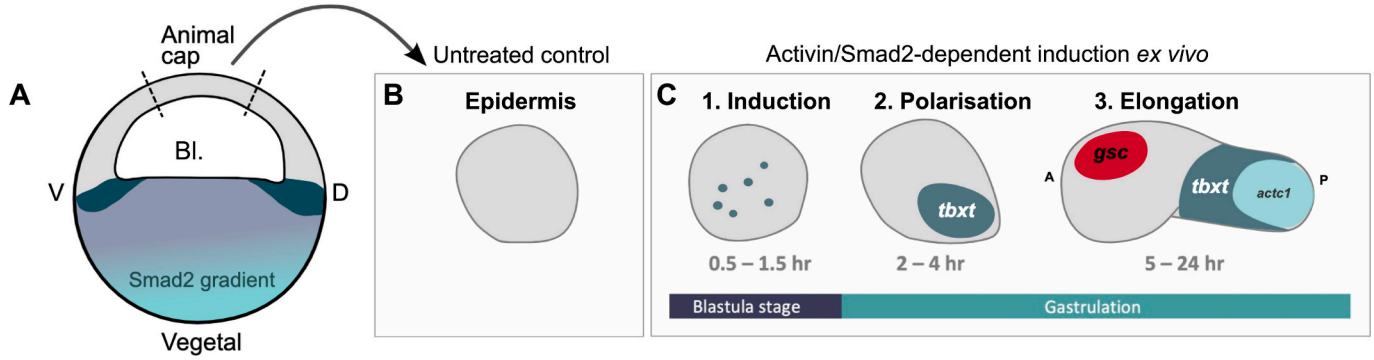

Fig. 1. Animal cap explant gastruloid induction assay *via* Activin treatment.
A) In the mid-blastula embryo, the animal cap tissue is separated from endogenous Activin/Smad2 signalling by the blastocoel (Bl.). B) Without Smad2 activation the animal cap tissue differentiates into epidermis *in vivo* and *ex vivo*. C) exposed to Activin animal cap explants are induced to form mesodermal tissues exhibiting convergence and extension driven elongation that express markers including *gsc*, *tbxt* or *actc1* and can therefore be used as a model of gastrulation morphogenetic and patterning events.

2.2. Mechanical stimulation through uniaxial compression leads to cell shape and nuclear deformation

To investigate the interplay of biochemical signals and mechanical forces in early germ layer specification, we used animal cap explants from mid-blastula *X. laevis* and applied mechanical stress through confinement between agarose and a glass-bottom culture dish (Fig. 2A). This setup allows treatment of intact explants with diffusible molecules combined with live imaging without attachment to a coated substrate. Compression was applied using a custom designed tool (Supplementary Movie 1) described previously (Srivastava et al., 2017). After contact with explants was visually established, we lowered the plunger 300 μm (±5.0 μm precision) at 0.2 mm/s which resulted in a compression that we characterised in terms of change in tissue area (Fig. 2B–C). The total explant area during compression was 100–250 % larger than before compression (Supplementary Movie 2) and the increase in area was maintained throughout the 1-hour confinement under agarose (Fig. 2D). For clarity, percentage area increase was calculated as the area once the plunger was lowered to its final position (area during compression, *e.g.* 0.531 mm^2) minus the initial explant area just before compression (*e.g.* 0.256 mm^2) divided by the initial area and expressed as a percentage (107 % area increase).

A dramatic decrease in explant area was observed immediately once the plunger was lifted. When initial area was set to 0 and beginning of compression to 1, area after lifting compression was observed to be 0.3 on average, suggesting that mechanical stress did not dissipate during the induction period (Fig. 2D). To determine the change in height, explants were imaged in MMR medium containing rhodamine-dextran (Fig. 2F–G). Reslicing the images allowed for comparison of explant height before and during compression (Fig. 2J) and calculation of average compressive strain in the z-axis ($\varepsilon = -0.65 \pm 0.04$, 95 % confidence interval).

To confirm that mechanical deformation at the tissue scale led to deformation at cellular and subcellular scales, explants co-labelled with membrane-EGFP and H2B-mCherry were imaged at a higher resolution. The cell and nuclear shape changes of the deep layer of the ectoderm were characterised using a single confocal section taken at each 50 μm increment in compression (0–350 μm). Using a combination of manual and automated segmentation approaches of an explant region revealed that a 300 μm applied compression led to a 32 % median increase in cell area (Fig. 3A). The effect size of compression on cell area was evaluated using the Cohen's d test where the difference in mean is divided by the standard deviation (Lakens, 2013). Using conventional effect size bounds we report a 'moderate' effect on cell area (Cohen's $d = -0.508$). This suggests that the increase in overall tissue area can be in part explained by cell area increase. However, at applied compression 0–100 μm where there is no cell area increase, the increase in explant area is likely due to flattening as the animal cap explant partially rounds up between dissection and compression (Dingwell and Smith, 2018). Another factor that has been observed throughout compression is the increase in the number of visible nuclei (Supplementary Fig. 2) which increases from 72.8 (SD = 15.8; at 0 μm compression) to 122 (SD = 8.7; at 300 μm compression), or by a factor of 1.7 (SD = 0.26).

Translocation of cells from other layers into the focal plane was also observed (Supplementary Movie 3). Segmentation of nuclear shape showed a median area increase of 15 % at 300 μm of applied compression (Cohen's $d = -0.383$, Fig. 3B). This suggests that subcellular compartments are deformed at higher levels of compression (300–350 μm). Nuclear deformation has been previously described to allow for alteration in the shuttling of transcription factors in response to

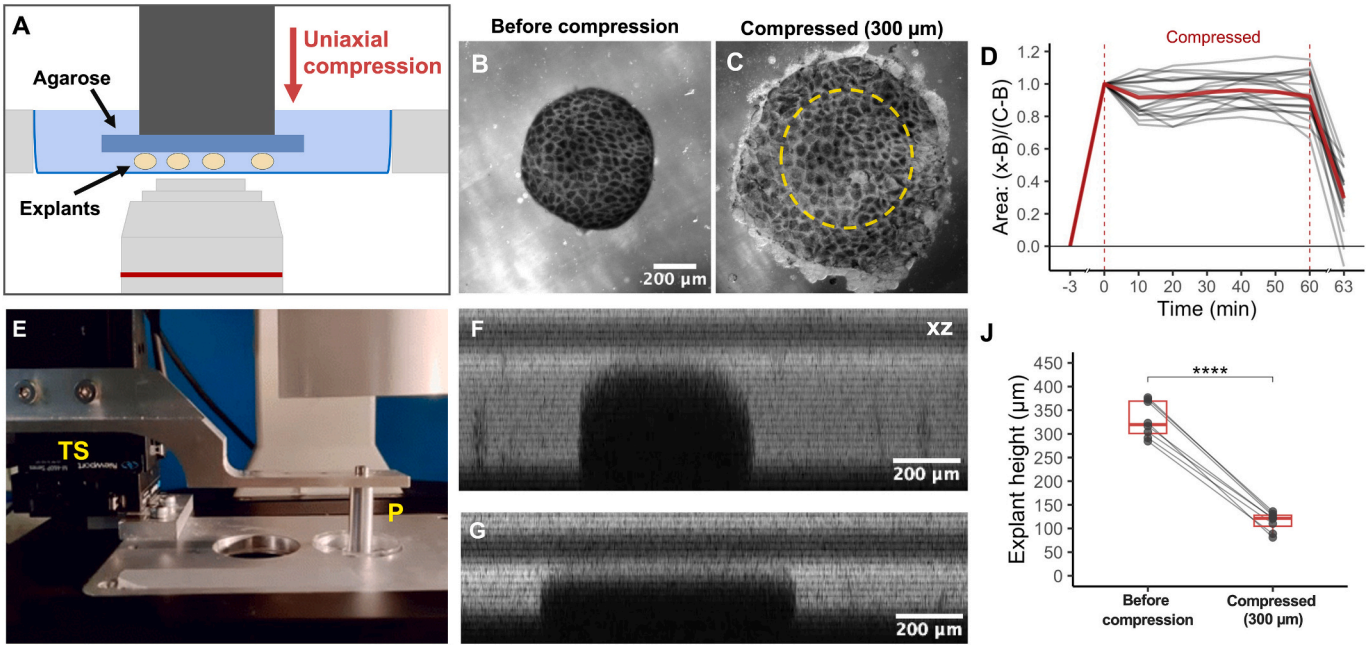

Fig. 2. Uniaxial compression as a method to mechanically stimulate intact explants. A) Schematic of compression set up with mechanical load applied with the use of a plunger (dark grey) resulting in explants being confined between agarose and culture dish glass. Set up is suitable for inverted microscope imaging (See Supplementary Fig. 1). B) Superficial side of an animal cap explant before compression is applied. C) The same explant was exposed to compression (plunger moved downwards by 300 μm from point of contact) resulting in an area increase of 175 %. The yellow circle outlines the explant before compression. D) Minimum-maximum standardised area (x) calculated as (x-B)/(C-B) where B is the area before compression (x = 0) and C is an area at the onset of compression (x = 100) at time 0. Compression was applied for 1 h with an area measurement every 10 min. The final time point ($t = 63$ min) is the area after the removal of confinement. The end of compression is marked by a vertical red line ($t = 60$ min). A horizontal line at standardised area 0 was added for reference. (total 26 explants in three independent experiments). E) Photograph of the compression tool set up fixed to the stage of an inverted microscope. TS = translational stage, P = plunger. F-G) An explant before and during compression imaged using a confocal microscope with fluorescent dextran in media (xz-plane view following re-slicing). J) Explant height decreases after compression (Welch Two Sample *t*-test, *p*-value = 2.917×10^{-8}, points represent individual explants). (For interpretation of the references to color in this figure legend, the reader is referred to the web version of this article.)

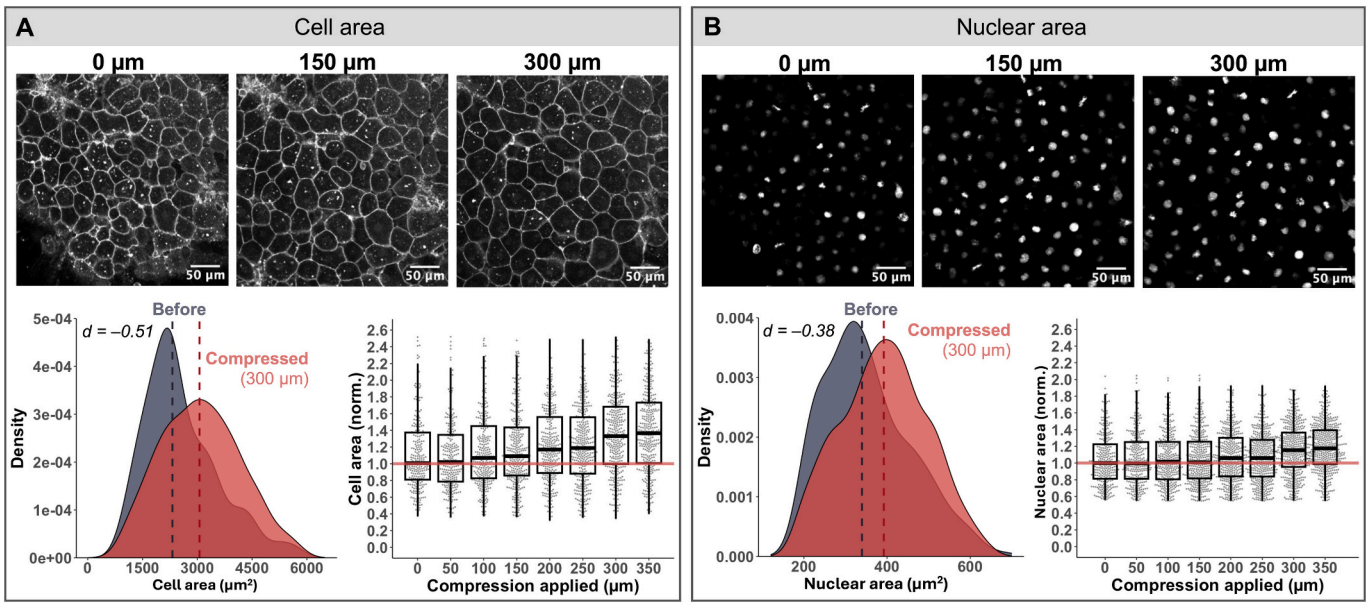

Fig. 3. Compression leads to cell area increase as well as nuclear deformation. A) Live imaging (mem-EGFP) of deep layer cells in an explant undergoing compression reveals deformation of cells with a 32 % increase (Cohen's d = −0.51) in segmented cell area at 300 µm applied compression and a gradual increase in median cell area with increasing extent of compression (at least 44 cells per time point in 4 separately compressed explants, points represent cells). B) Analysis of nuclei (H2B-mCherry) during compression (300 µm) shows a 15 % increase in nuclear area (Cohen's d = −0.38) with the mean number of segmented nuclei per explant increasing from 72 to 112 from 0 to 300 µm compression (at least 56 nuclei per time point in 4 separately compressed explants, points represent nuclei).

mechanical cues (Elosegui-Artola et al., 2017; Skory et al., 2023). Taken together these results show that uniaxial compression is sufficient to systematically induce mechanical deformation of cells in animal cap explants.

2.3. Elongation of animal cap gastruloids is reduced following compression during Activin induction

To investigate the interaction between mechanical stimulation and biochemical inputs, animal cap explants were induced with Activin, a well characterised system for mesodermal induction *ex vivo* (Ninomiya et al., 2004; Green et al., 2004; Moris et al., 2020). To test whether mechanical cues can affect Activin-dependent induction, explants dissected from mid-blastula embryos (Stage 8.5) were exposed to uniaxial compression sufficient to produce at least a 100 % area increase during the time of induction (Fig. 4A–D). Explants were then imaged after 20–24 h when sibling embryos reached a late gastrulation stage at the onset of neurulation (Stage 12.5). To accurately assess the elongation of explants, an elongation index (EI) was devised where the explant's midline is divided by the diameter of the largest fitted circle (Fig. 4E). The elongation index performed better than other measurements such as aspect ratio as the midline measurement more accurately measures explant length when the elongation axis is curved.

Uninduced explants remain as spherical epidermal tissue (Fig. 4B). In explants that were treated with Activin alone (10 ng/mL), elongation is observed as expected (Ninomiya et al., 2004; Ariizumi et al., 1991); however, the elongation index is significantly reduced (*t*-test, $p = 2.072 \times 10^{-6}$) when compression is applied for 1 h between 0.5 and 1.5 h of the induction period (Fig. 4C–F). Compressing for 1 h after the period of induction did not lead to an inhibition of elongation (Fig. 4E) with an elongation index not significantly different to Activin-only controls (*t*-test, $p = 0.961$). This means that compressed explants can fully elongate and suggests that mechanical stimulation directly affects the process of induction and not later morphogenesis.

2.4. Mechanical stimulation of animal cap gastruloids affects mesodermal axial marker expression and promotes head Organiser induction ex vivo

The loss of elongation observed in response to mechanical compression might be explained by the inhibition of mesoderm induction. Therefore, to investigate whether fate choice is affected by mechanical stimulation of induced explants, a gene expression analysis was performed using established markers for ectoderm and mesoderm involved in early development as well as animal cap explants (Satou-Kobayashi et al., 2021; Briggs et al., 2018). The pan-mesodermal marker *tbxt* was highly upregulated in Activin treated samples when compared to uninduced control at 3 h post-induction (Fig. 5A). However, compressed Activin-induced explants showed a high level of *tbxt* expression, suggesting that mesoderm induction is not inhibited by mechanical stimulation (Mann-Whitney *U* test two-sided, *p*-value = 1, Fig. 5A).

An alternative explanation for elongation loss could be the induction of a different type of mesoderm. Indeed, it has been observed that Activin exhibits dose dependency where low doses lead to ventral mesodermal (VM) specification and high doses result in explants composed of mainly dorsal notochord tissue. Previous studies have shown that both these tissue types have reduced elongation when compared with dorsal mesoderm obtained from the 1.5 h 10 ng/mL Activin treatment (Ariizumi et al., 2017; Ariizumi et al., 1991; Gurdon et al., 1993). The ventral mesoderm markers *vent1* and *wnt8* (*wnt8a*) have not increased when comparing Activin-treated explants with and without compression. A small reduction in the mean fold change was observed for both *vent1* and *wnt8* in explants exposed to compression (Mann-Whitney *U* test, one-sided, *p*-value = 0.032, Fig. 5B–C). Importantly, markers specific for dorsal mesoderm – which gives rise to the leading edge (LEM), pre-chordal (PCM) and chordal (CM) mesoderm tissue types – were highly increased upon compression (Mann-Whitney *U* test, one-sided, p-value = 0.032, Fig. 5D–E). At early gastrula this tissue corresponds to the Organiser, with the markers *chordin* (*chrd*), *cerberus1* (*cer1*) and *goosecoid* (*gsc*) being the most highly upregulated genes. Specifically, this means an average fold change from Activin-only samples of >5 and an average fold change from uninduced control of at least 200 times. Further head Organiser markers, including *gata4*, *otx2*

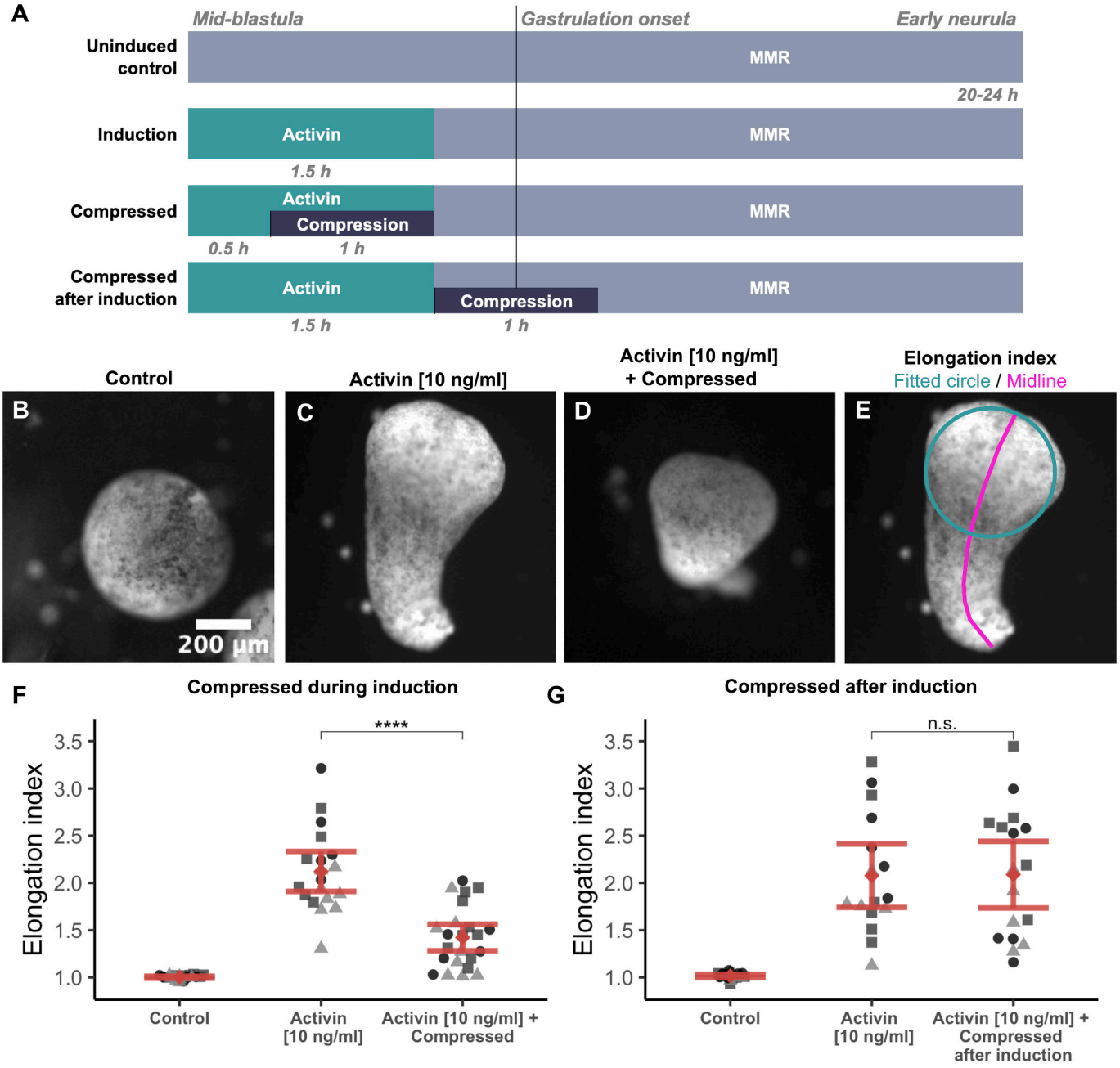

Fig. 4. Elongation of animal cap explants treated with Activin is lost when compression is applied during induction. A) Diagram illustrating the timing of application of compression and Activin A treatment in explants dissected at mid-blastula stages and kept until sister embryos reached early neurula (Stage 13) in MMR (Marc's Modified Ringer's culture media). B) Untreated, intact explants remain spherical during the first day of culture (Elongation index (EI) close to 1.0 ± 0.01, 95 % confidence interval). C) An intact explant treated with Activin A (10 ng/mL) for 1.5 h exhibits elongation driven by the convergence and extension characteristic of dorsal mesoderm (Elongation index = 1.8). D) Elongation is significantly reduced in Activin-treated explants when exposed to compression during induction (Elongation index = 1.2). E) Elongation was quantified using an 'Elongation index' where the midline (magenta) is divided by the diameter of the largest fitted circle (cyan). F) The elongation index is measured as the ratio of the midline (orange) divided by the diameter of the largest fitted circle (red). E) The elongation index of Activin induced explants is significantly reduced in combination with compression (Welch Two Sample *t*-test, $p = 2.072 \times 10^{-6}$, $n > 6$, 3 independent experiments) G) The elongation index is not significantly reduced when compression is applied after the 1.5 h Activin induction period (Welch Two Sample *t*-test, $p > 0.961$, $n > 5$, 3 independent experiments). (For interpretation of the references to color in this figure legend, the reader is referred to the web version of this article.)

and *sox17b* were also increased when compared to uninduced controls within the range between 7 and 22-fold.

Upregulation of *cer1* and *gata4* suggests that mechanically stimulated explants contain more anterior head Organiser tissue (Bright et al., 2021; Briggs et al., 2018). Head Organiser identity is consistent with the observed loss of elongation (Fig. 3), as the anterior dorsal mesoderm elongates less than the posterior dorsal mesoderm in part because of the production of signals (*e.g.* anti-Wnts) that lead to the inhibition of convergence and extension (Cornell and Kimelman, 1994; Guger and Gumbiner, 1995; Huang and Niehrs, 2014). Upregulation of *gsc* alone has been reported to disrupt Wnt/PCP signalling and reduce elongation in embryos and dorsal marginal zone (Keller) explants (Ulmer et al., 2017).

The superficial ectoderm marker *xk81a* (*epidermal keratin*) was expressed in all explants (Fig. 6A), which is consistent with the lack of response to Activin treatment observed in superficial cells (Green, 1999;

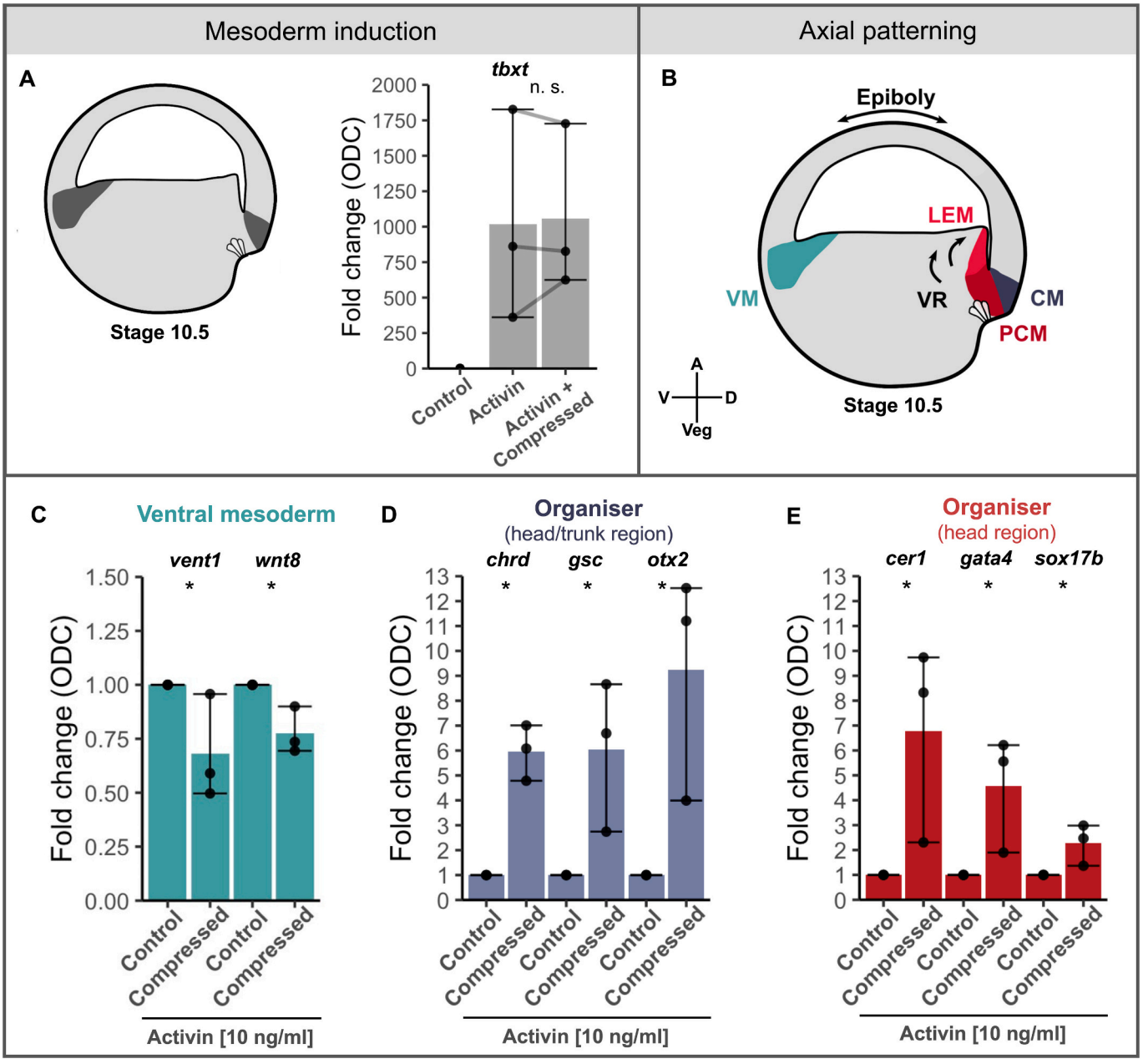

Fig. 5. Compression leads to an increase in head organiser marker expression. Explants induced at mid-blastula (Stage 8.5) were allowed to develop until sibling embryo Stage 10.5 (early gastrulation), illustrated here in a cross section with endogenous pan-mesoderm marker *tbxt*. A) Expression of pan-mesodermal marker (*tbxt*) induced by Activin (10 ng/mL) is not affected by compression. Fold change relative to uninduced control. B) Mesodermal axial patterning in gastruloids is affected by compression. The cross section shows different types of mesoderm found at Stage 10.5 (VM = ventral mesoderm, CM = chordal mesoderm, PCM = pre-chordal mesoderm, LEM = leading-edge mesoderm). C) At 3 h post-induction ventral mesoderm markers *vent1* and *wnt8a* show a decrease in in induced explants with compression compared to non-compressed explants. Fold change from intact Activin-treated controls is shown. D) Markers expressed in the head and trunk regions of the early gastrula organiser (*chrd*, *gsc* and *otx2*) are upregulated upon compression. E) Markers expressed in the head region but not the more posterior part of the organiser (*cer1*, *gata4*, *sox17b*) are also increased in compressed-induced explants. Average of 10 explants with error bars showing the range and points represent individual experiments ($N = 3$). Plot p-values: n. s. ≥ 0.05, * < 0.05 (Mann-Whitney U test, one-sided).

Ariizumi et al., 1998). Uninduced control animal cap explants did not express mesodermal markers when compared with Activin treated explants (Fig. 6C) except *vent1* which has been reported to be expressed in deep ectoderm cells in the embryo blastocoel roof (Bright et al., 2021; Sander et al., 2007). We observed a high level of variation in some upregulated genes and asked whether the increase in relative expression is associated with some parameter that varies between experiments. Interestingly, when considering the median area increase before and at initial compression in individual experiments the expression of head Organiser markers, including *gsc* and *chrd*, increases proportionally to mechanical stimulation (Fig. 6B). All dorsal mesoderm markers follow this trend, whereas the ventral marker *wnt8* is highest at the lowest area change upon compression (Fig. 6C). This suggests that variation in gene expression and elongation between experimental runs is at least partially a result of variation in the extent of the mechanical input.

Taken together, analysis of gene expression after Activin induction has revealed that mechanical stimulation by compression leads to an increase in Organiser marker expression and particularly a shift toward head mesoderm. This means that the observed reduction in elongation is not caused by an inhibition of mesoderm induction itself but rather a

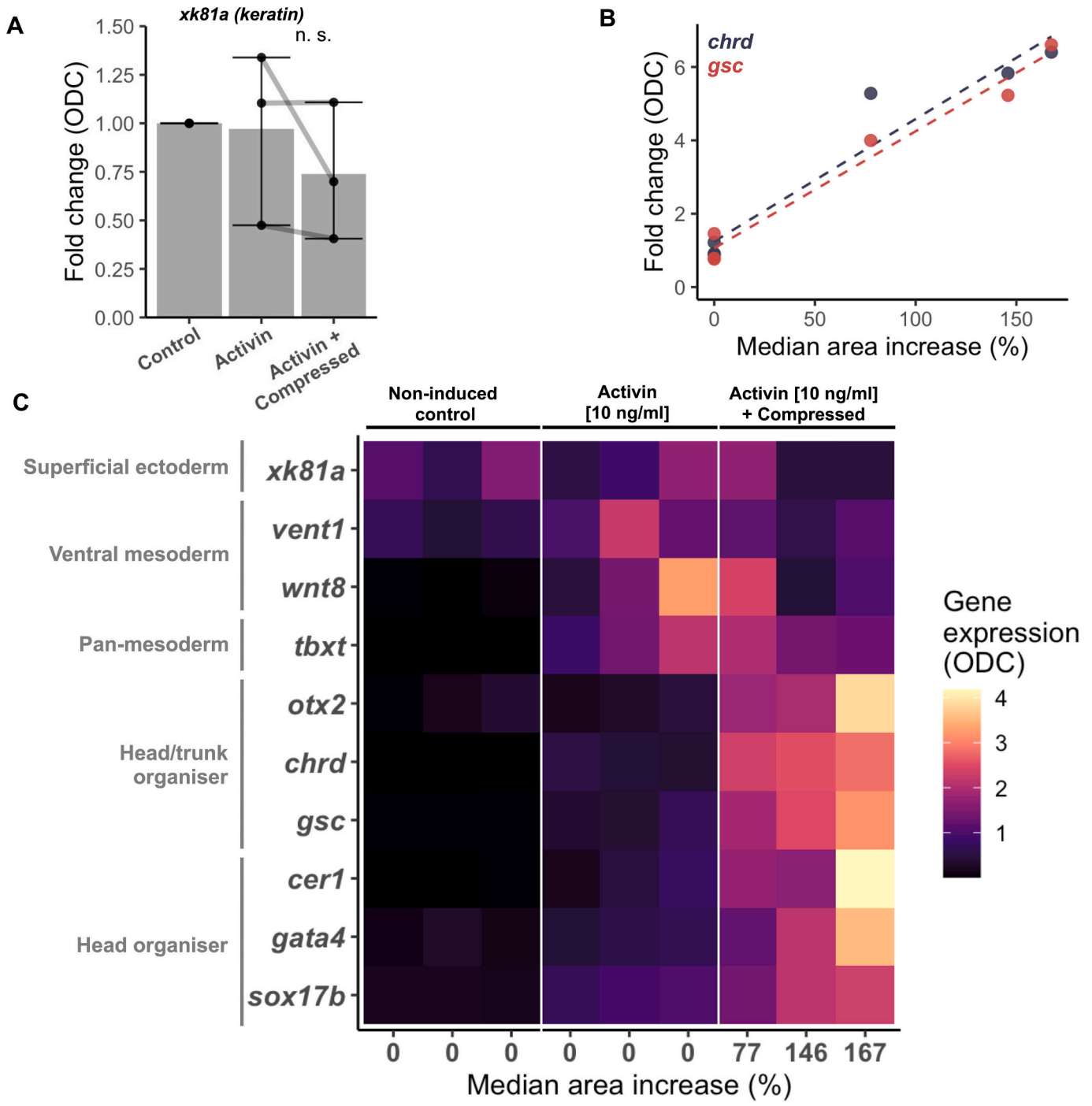

Fig. 6. Patterns of gene expression in mechanically stimulated induced explants. A) Animal cap superficial layer marker *keratin* (*xk81a*) was not significantly affected by Activin (10 ng/mL) treatment nor by combined stimulation with Activin and compression. Fold change normalised by respective non-induced control (Mann-Whitney *U* test, one-sided, $p = 0.663$, points represent individual experiments, error bars show range, normalised to *ODC* in 3 independent experiments). B) Results of individual RT-qPCR samples (points represent Activin and Activin + Compressed conditions from 3 independent experiments, 10 explants each) imply a relationship between organiser gene expression (fold change from Activin-treated samples, normalised to *ODC*) and the extent of mechanical stimulation (expressed as median area increase in percentage). C) Heatmap of fate marker gene expression quantified as $2^{-\Delta Ct}$ normalised by mean of all samples to show relative changes in expression. Left column: non-induced control explants; Middle: Activin (10 ng/mL) treated explants; Right column: Activin-treated explants exposed to compression ordered by median area increase (%) from low to high (N = 3 experiments).

change in mesodermal fate determination.

2.5. β-Catenin stabilisation during induction is sufficient to reduce elongation and upregulation of a dorsal anterior marker

To establish a mechanism by which mechanical compression leads to an increase in head Organiser marker expression, we considered pathways that are both involved in Organiser formation in the embryo as well as known to be responsive to mechanical stimulation. The most promising was the Wnt/β-catenin pathway, as its role in Organiser induction *in vivo* is well established (Crease et al., 1998; Ding et al., 2017; Kiecker and Niehrs, 2001), and previous work has shown that β-catenin

is mechanosensitive (Muncie et al., 2020; Röper et al., 2018; Pukhlyakova et al., 2018). We therefore tested β-catenin as a possible candidate for the mechanoresponsive activity of animal cap explants.

First, we investigated whether activation of β-catenin during the 1.5 h Activin induction could have a similar effect on gastruloid development as compression. For dose and temporal control of β-catenin activation, the GSK3α/β pharmacological inhibitor BIO was used as at later stages Wnt/β-catenin signalling inhibits anterior mesoderm and neural structures (Hikasa and Sokol, 2013). Activation of Wnt/β-catenin by adding 5 μM BIO to Activin (10 ng/mL) treated explants is sufficient to reduce elongation after 24 h (*t*-test, $p = 1.505 \times 10^{-5}$, Fig. 7A–D). The amount by which elongation is reduced is similar when compared to compressed induced explants (Fig. 7E). We then analysed the expression of mesodermal markers using RT-qPCR (Fig. 7F–G). Wnt/β-catenin activation through BIO leads to the upregulation of *cer1*, a marker for the most anterior region of the Organiser, whereas the pan-mesodermal marker *tbxt* remains at a similar level when compared with Activin only samples. Therefore, the effect of compression on both elongation and Organiser marker expression can be reproduced using β-catenin activation alone.

2.6. β-Catenin is stimulated by compression and required for mechanics-dependent Organiser induction in gastruloids

Next, we tested whether compression is sufficient to activate Wnt/β-catenin signalling. Explants were compressed for 1 h with Activin (10 ng/mL) and stained using an antibody against total β-catenin (Fig. 8A–C) which showed an increase in β-catenin nuclear signal normalised to cytoplasmic intensity (*t*-test, $p = 0.024$). An increase in the nuclear to cytoplasmic ratio suggests higher β-catenin nuclear activity in mechanically stimulated cells.

We then asked whether β-catenin activity is required for the effect of compression on marker expression downstream of the β-catenin signalling pathway. Previous studies have shown that Wnt inhibition after induction leads to a reduction of anterior mesoderm (Kiecker and Niehrs, 2001; Itoh and Sokol, 1999), to avoid this confounding effect on later mesoderm specification, we measured the expression of the earliest response gene *sia* (*siamois*), which is known for its role in the activation of head Organiser markers (*gsc*, *chrd*) and requires β-catenin and Smad2 for transcriptional activation (Crease et al., 1998; Ding et al., 2017). In compressed samples *sia* expression was increased at 0.5 h after Activin induction (Mann-Whitney *U* test, one-sided, *p*-value = 0.011) in line with the effect of compression on head Organiser gene expression (Fig. 8D). We then tested whether β-catenin is necessary for *sia* activation by mechanical stimulation. To degrade β-catenin, explants were treated with the small molecule IWR-1 during induction. IWR-1 is a Tankyrase inhibitor which prevents the ubiquitination of Axin2, stabilising the β-catenin destruction complex (Dyer et al., 2015). Expression of *sia* was rescued (Mann-Whitney *U* test, one-sided, p-value = 0.040) in compressed explants that were treated with IWR-1 [40 μM] during induction with Activin (Fig. 8E).

The correct length of the *siamois* product (170 bp) was confirmed

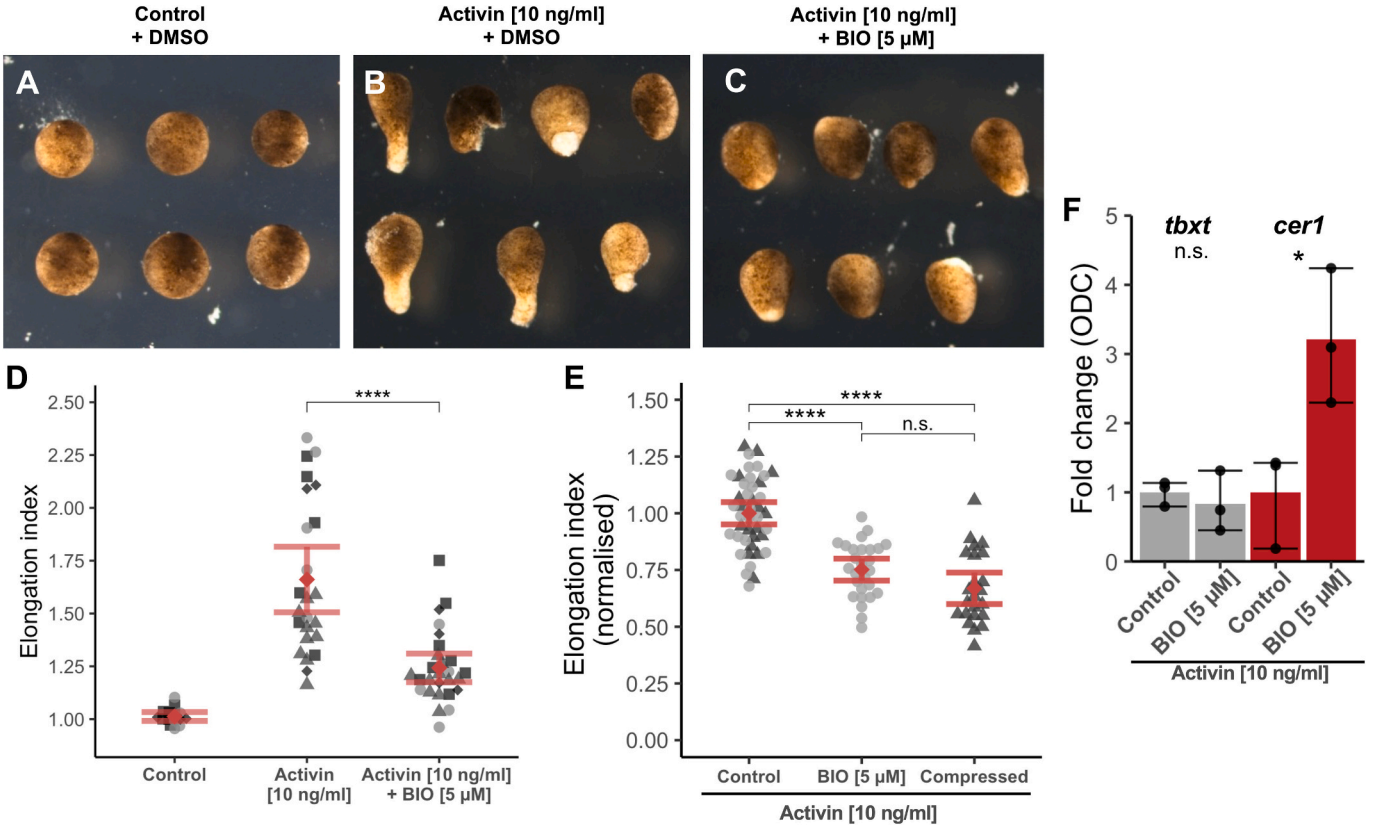

Fig. 7. β-catenin stabilisation through BIO treatments leads to head organiser gene expression and reduction of elongation. A) Control explants with DMSO cultured for 24 h after induction. B) Activin-treated explants (10 ng/mL) with DMSO for 1.5 h. C) Explants exposed to both Activin (10 ng/mL) and BIO (5 μM) to stimulate Wnt/β-catenin signalling during induction. D) Quantification of the elongation index of explants, 5 μM BIO treatment leads to a significant reduction in elongation of induced explants (Welch Two Sample *t*-test: $p = 1.505 \times 10^{-5}$, at least 5 explants per condition, 4 independent experiments represented by different point symbols). E) The degree of elongation reduction by BIO was compared to mechanical stimulation. The difference in elongation index normalised to the mean of elongation index of the Activin control in the corresponding experiment is not significant between BIO treated and compressed explants. (One-factor Anova, Tukey HSD *post hoc* test, point symbol represents either BIO or compression experiments). F) RT-qPCR analysis of expression after 3 h post induction shows that Wnt/β-catenin activation through BIO leads to an increase in *cer1* (Mann-Whitney *U* test, one-side, $p = 0.0404$), an anterior head organiser marker expression without affecting *tbxt* expression (Mann-Whitney *U* test, two-sided, p = 0.663). Pool of 10 explants, points represent independent experiments, $N = 3$.

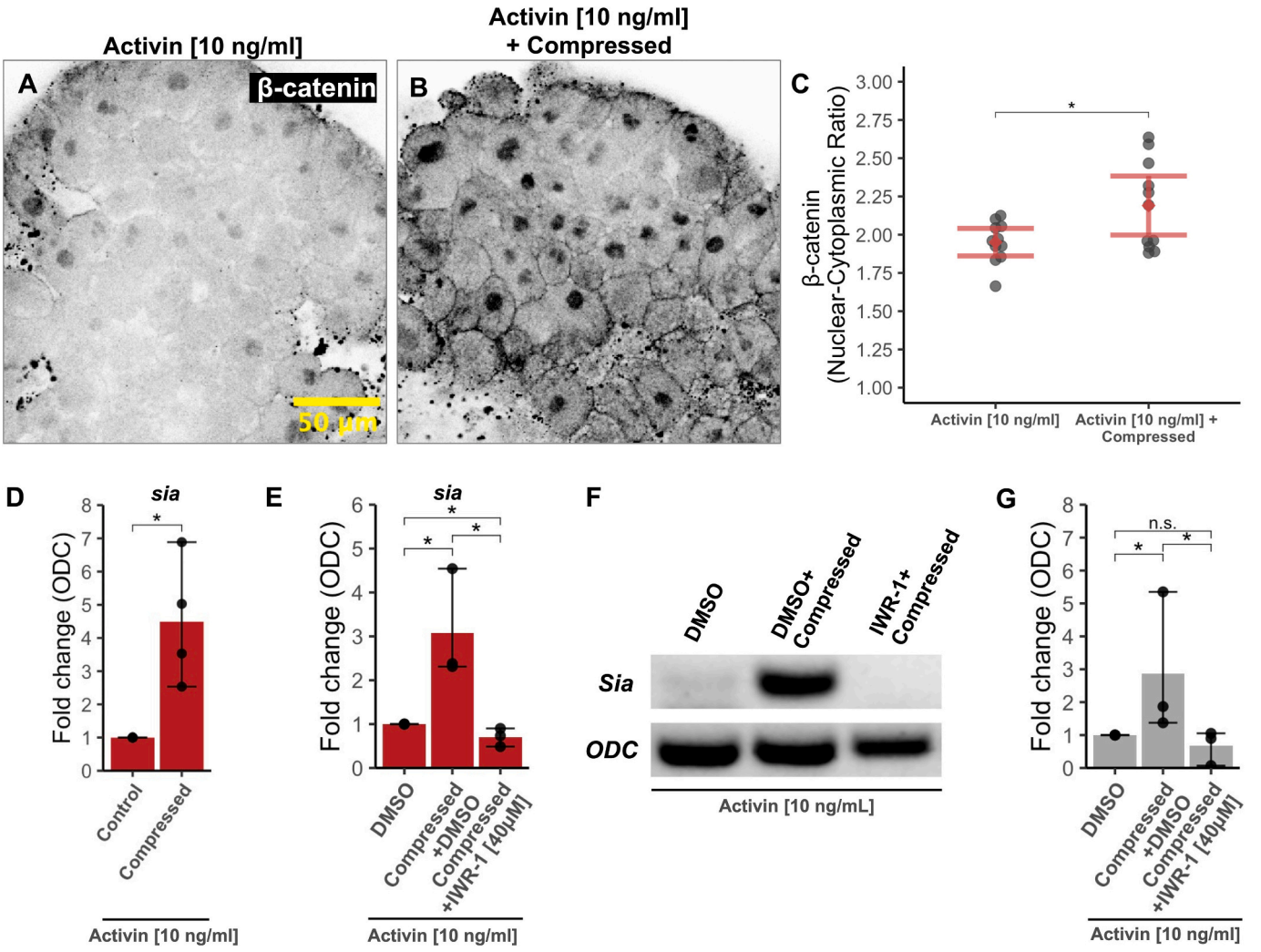

Fig. 8. β-catenin activation upon compression in Activin treated explants and its effect on *sia* expression. A–B) Immunostaining showed β-catenin is increased in animal cap explants after 1 h of compression compared with intact control explants. All explants were exposed to Activin (10 ng/mL). C) Nuclear to cytoplasmic ratio quantification showed a significant increase of β-catenin nuclear localisation in compressed explants. Points represent averages of at least 20 deep layer cells (total = 662 cells) of individual explants (Welch Two Sample *t*-test, $p = 0.024$; 11 explants in each condition; N = 3). D) RT-qPCR analysis at 30 min post induction showed that compression during normal induction (1.5 h with 10 ng/mL Activin) leads to an increase in *siamois* (*sia*) expression (Mann-Whitney *U* test, one-sided, $p = 0.011$, 5–10 explants pooled, $N = 4$). E) This effect of compression was inhibited when β-catenin degradation was stimulated using IWR-1. Thereby tissue mechanics-dependent *siamois* activation was rescued by Wnt inhibition. (Pair-wise comparisons: Mann-Whitney *U* test, one-sided, $p < 0.05$; Kruskal-Wallis rank sum test, p = 0.024; 5–10 explants pooled; N = 3). F) Results from a DNA electrophoretic gel of the RT-PCR products shown in panel E used to confirm correct product size. Top row: *siamois*, Bottom row: *ODC*. G) Mean grey value of electrophoretic gel bands, *siamois* normalised to *ODC*, points represent fold change from Activin-only condition (pair-wise comparisons: Mann-Whitney *U* test; Kruskal-Wallis rank sum test, $p = 0.055$).

using an electrophoretic DNA gel with the *sia* and *ODC* RT-qPCR products. Quantification of band signal intensity using the background-subtracted mean grey value normalised to *ODC* showed a similar trend to the RT-qPCR results (Fig. 8F–G), although the difference between Activin and Activin with compression and IWR-1 was no longer significant (Mann-Whitney *U* test, one-sided, p-value = 0.321). Note that the RT-qPCR product is the final amount of DNA after the PCR reaction and is not reflective of initial RNA levels.

Taken together, these results support the model that compression leads to an increase in β-catenin nuclear activity that leads to increased head Organiser gene expression. Transient pharmacological stimulation of β-catenin activity has a similar effect on Activin induced explants by inhibiting elongation and activating Organiser gene expression. Wnt/β-catenin activation is both necessary and sufficient for the effect of compression on *siamois* expression, a key transcription factor involved in Organiser induction.

3. Discussion

The role of mechanical forces in instructing the fate and behaviour of cells in embryonic tissues has become appreciated in the last decade (De Belly et al., 2022; Piccolo et al., 2022; Miller and Davidson, 2013). Previous studies have linked mechanical tension with mesoderm formation in different systems including *Drosophila*, zebrafish and human embryonic stem cells (Brunet et al., 2013; Muncie et al., 2020). However, how morphogen signals interact with mechanical stimuli is still poorly understood.

Here we present an experimental system, where mechanical stimulation is combined with biochemical induction in the form of uniaxial compression and Activin treatment. This allowed the investigation of the interplay of mechanics and morphogen signalling directly with high temporal control of both stimuli in primary embryonic explants without introducing confounding variables such as substrate attachment or disaggregation. The fast development of *X. laevis* compared to

mammalian systems allows for relatively short induction times (*e.g.* 1.5 h) and this assay could be used to test new hypothesis that relate to different molecular and mechanical cues.

We further showed that mechanical stimulation modulates Activin signalling by increasing β-catenin activity which leads to the induction Organiser genes such as *cerberus 1*, *goosecoid* and *chordin* (Figs. 5–6 and 8). Compression of animal cap explants stimulated with Activin leads to the reduction of elongation characteristic of the trunk and posterior dorsal mesoderm (Fig. 3). We show that compression can both increase β-catenin nuclear enrichment and that the effect of compression on *siamois* expression – a key transcription factor required for the β-catenin-dependent Organiser induction – is abolished when β-catenin is degraded. Furthermore, β-catenin activity alone during Activin induction is sufficient to reproduce the effects of compression. Taken together these results suggest a role of compression in the β-catenin-dependent activation of head Organiser genes (Fig. 8).

Mechanical deformation of cells has been reported to activate β-catenin signalling through several mechanisms including membrane and cytoskeleton deformation (Röper et al., 2018; Gayrard et al., 2018) and through nuclear deformation by affecting mechanoresponsive pathways such as Hippo/Yap signalling (Deng et al., 2018; Benham-Pyle et al., 2015). Both cell shape and intracellular (nuclear) mechanical deformation have been observed during uniaxial compression of animal cap explants which could be sufficient to activate β-catenin through these reported mechanisms (Fig. 3). Compression of explants has also caused a substantial thinning of the tissue (Fig. 2F–J) and an increase in visible nuclei suggesting intercalations (Supplementary Fig. 2). These cell-cell rearrangements could lead to additional mechanical tension and remodelling of cell-cell adhesion. Cadherins are known to directly affect β-catenin localisation when mechanically engaged (Röper et al., 2018; Benham-Pyle et al., 2015). This makes C-cadherin, the type expressed at early stages of *X. laevis* development, an interesting candidate for mechanotransduction with β-catenin having been reported to be antagonised by C-cadherin binding (Fagotto et al., 1996).

The observation that mechanical forces contribute to Organiser establishment in Activin induced explants suggests that a similar mechanism could be possible *in vivo*. It is broadly accepted that β-catenin accumulation in the dorsal side of *X. laevis* embryos is a consequence of cortical rotation and directly leads to the establishment of the blastula *chordin* and *noggin* expressing centre (sometimes termed pre-Organiser) as well as the Spemann-Mangold Organiser proper through the overlap of Activin/Nodal and β-catenin activity according to the 3-signal model of mesoderm induction (Ding et al., 2017; Ishibashi et al., 2008; Kuroda et al., 2004). However, it has been previously described that some of the

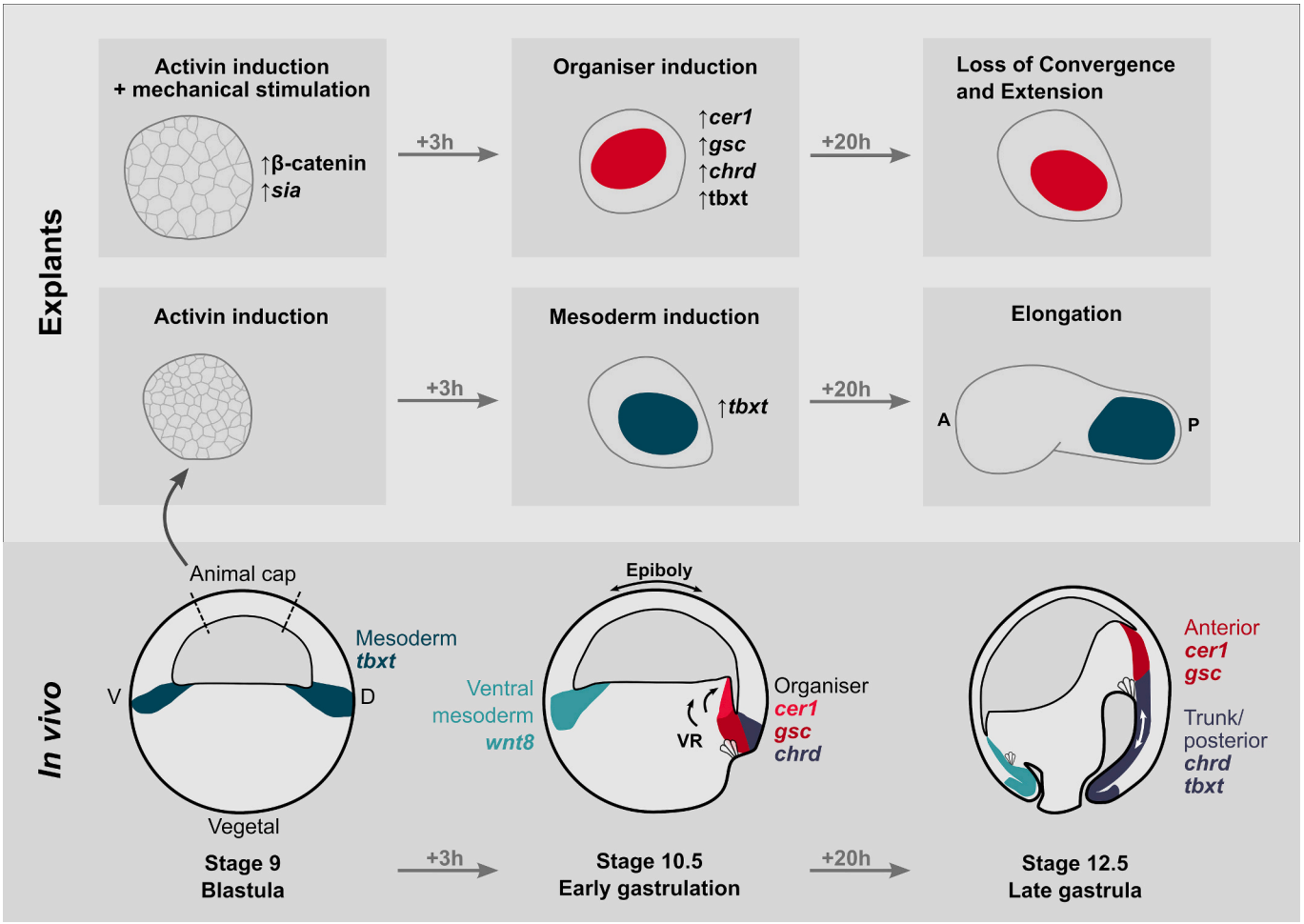

Fig. 9. Tissue mechanics modulate Activin-dependent mesoderm induction and promote the formation of the head organiser *ex vivo*. Schematic representation of the main findings of this work. Explants derived from the blastula animal cap can be induced *ex vivo* using Activin and recapitulate aspects of early mesoderm morphogenesis by elongation through convergence and extension (C&E) and fate specification by expression of markers of a variety of mesodermal derivatives along the antero-posterior axis. When exposed to mechanical stimulation through compression and confinement, Activin-induced animal cap explants show increased nuclear β-catenin activity followed by activation of a Wnt-dependent transcription factor *siamois* (*sia*). The later expression shows an increase in Spemann-Mangold organiser markers including *cerberus 1* (*cer1*), *goosecoid* (*gsc*) and *chordin* (*chrd*) in compressed explants compared with intact explants which suggest the loss of elongation upon compression is due to the formation of more anterior dorsal mesoderm.

early β-catenin nuclear signals during early gastrulation movements cannot be explained by dorsal accumulation of maternal dorsal determinants and appear too early for zygotic *wnt8* activity (Schohl and Fagotto, 2002; Schohl and Fagotto, 2003). We speculate that β-catenin nuclear activity in mid to late blastula stages surrounding the blastocoel could be explained through the effect of mechanical stimulation by either the expansion of the blastocoel cavity and associated increase in hydrostatic pressure (described recently (Alasaadi et al., 2024)) or by force-generating morphogenetic movements.

Indeed, the cell population that gives rise to the Organiser experiences one of the first major morphogenetic movements in development and is likely uniquely affected by the mechanics of the pre-gastrulation embryo (Bruce and Winklbauer, 2020; Kaneda and Motoki, 2012). The presumptive head Organiser cells (positioned near the blastocoel cavity) move toward the vegetal pole of the embryo and involute mainly by the combined action of the presumptive ectoderm epiboly and vegetal rotation (see Stage 10.5, Fig. 9) (Bauer et al., 1994). We have observed that both cell area and intercalation are increased during compression of animal cap explants. The force generation resulting from vegetal cell movements intercalation is sufficient to fold the most anterior part of the Organiser and push it against the blastocoel wall (Winklbauer and Parent, 2017; Wen and Winklbauer, 2017) and could be a source of mechanical stimulation *in vivo*.

Based on these observations, we propose that the presumptive Organiser cells could be exposed to mechanical deformation from surrounding force-generating cell populations sufficient to affect the establishment of spatial patterning of Organiser gene expression. Given the role of β-catenin-dependent signalling in specifying the vertebrate dorsal organisers is highly conserved and coincides with early large-scale morphogenetic movements, it is conceivable that mechanical stimulation plays a role in head Organiser induction or refinement of the anterior domain along with diffusible molecular signals. Future studies should investigate the possibility that head Organiser induction and its robustness are affected by mechanical cues *in vivo*.

4. Materials and methods

4.1. Obtaining and microinjecting Xenopus laevis oocytes

All work involving live adult animals (*Xenopus laevis*) was approved and done in accordance with the Home Office Project License at University College London. UK Home Office ethics guidelines and related regulations were followed. Oocytes were obtained as previously described (Shellard et al., 2018; Pearl et al., 2017). Adult *X. laevis* females were induced with 100 μL pregnant mare serum gonadotrophin hormone (equivalent to 100 IU, PMSG, Intervet) followed by injection of 250 (±50) μL chorionic gonadotrophin (equivalent to 500–750 IU Chorulon, Intervet). *In vitro* fertilisation of oocytes was performed using testes provided by the European Xenopus Resource Centre (EXRC). Jelly was removed using 1 g L-cysteine (Sigma-Aldrich) in 50 mL distilled water with 500 μl 5 N NaOH. Embryos were cultured in 0.1× Marc's modified Ringer's media (MMR) and dissected in 3/8 normal amphibian media (NAM) in plastic untreated culture dishes. Staging was done using the Nieuwkoop and Faber embryonic stage series (Nieuwkoop et al., 1994).

Injection of 2-cell or 4-cell embryos was carried out using the Narishige IM300 microinjector as previously described (Shellard et al., 2018). All blastomeres were injected with 200–400 pg mRNA in a 5 nL nuclease free water solution using a pulled glass capillary. Nuclear H2B-mCherry and Membrane-EGFP constructs were used and developed previously (Theveneau et al., 2010). Transcription *in vitro* was used to produce mRNA for injection. Appropriate New England Biolabs restriction enzymes and buffer mixtures were used for linearisation followed by transcription using the mMessage mMachine Kits (SP6, AM1340 and T7, AM1344, Thermo Fisher) according to manufacturer instructions. The RNA product was purified using the Monarch RNA Clean-up kit (T2040, New England Biolabs).

4.2. Micromanipulation and explant procedure

To produce gastruloids explants were dissected from the animal cap (AC) of Stage 8.5 embryos (Nieuwkoop et al., 1994). In brief, vitelline membrane removal and dissection were carried out using fine forceps (Dumont No. 5, 500342, World Precision Instruments). Presumptive ectoderm explants were dissected as a circle of approximately 500 μm in diameter with its origin at the animal pole following previously established protocols (Ariizumi et al., 2017; Green, 1999). Intact uninduced explants were kept as a control for lack of contamination with non-ectodermal cells.

In all experiments involving AC explant-derived gastruloids, induction was performed as follows: Intact explants containing both deep and superficial layers were placed in 0.7× MMR culture medium with 0.1 % BSA (R3960, Promega) and 10 ng/mL Activin A (a4941, Sigma) with the competent deep layer cells facing away from the hard substrate of the culture dish. After 1.5 h of induction, explants were washed 3 times and cultured in 0.7× MMR (Dale and Slack, 1987; Ariizumi et al., 2017; Dingwell and Smith, 2018; Sive et al., 2000).

Commercially available small molecules BIO (6-bromoindirubin-3′-oxime, B1686, Sigma) and IWR-1 (IWR-1-endo, Selleckchem, S7086) were used to activate or inhibit the canonical Wnt/β-catenin pathway. For animal cap explant treatment either 5 μM BIO or 40 μM IWR-1 were added to culture media used for Activin A induction. Control samples were exposed to a corresponding volume of dimethyl sulfoxide (DMSO, 5.89569, Sigma).

In mechanical stimulation experiments, a custom tool was used for uniaxial compression followed by confinement of explants. The design of the compression tool has been characterised previously (Srivastava et al., 2017). In brief, a microscope insert is attached to a translational stage set up (2×, M-460P Series, Newport) that connects an aluminium plunger with a motorised actuator powered through a DC servo motor (TRA25CC, Newport). The translational stages allow for manual x and y position adjustments. The actuator is controlled using a motion controller (SMC100, Newport). To compress explants, the tissue was placed under a thin block of agarose (1 % agarose, BP1356, Fisher BioReagents, in 0.7× MMR, dimensions: 5 × 5 mm and a height of 150 μm) to reduce deep layer cell-substrate attachment and prevent impeding liquid media access to the cell surface by direct contact with a hard impermeable substrate. Once the plunger/agarose came into direct contact a 'before' compression image was acquired followed by lowering the plunger by 300 μm to achieve an explant area increase of at least 100 % which is equivalent to a compressive strain of $\varepsilon = -0.65$ (based on resliced profiles of compressed AC in Supplementary Fig. 1). For live imaging of deep layer cells an identical set up was used except explants were inverted to enable visualisation of deep layer cells as pigment and yolk prevents imaging through the explant.

4.3. Detection of RNA and proteins

Extraction of total RNA from *X. laevis* samples was performed using the TRIzol reagent (15,596,026, Invitrogen) following manufacturer-provided protocol. RNA was extracted from 10 explants per experimental group and used directly following the Luna Universal One-Step RT-qPCR Kit (E3005, New England Biolabs) protocol. Alternatively, RNA was used to synthesise complementary DNA using the First Strand cDNA Synthesis Kit (K1612, Thermo Fisher) and analysed using the SYBR Green Master Mix (A25742, Applied Biosystems). Quantitative-PCR (RT-qPCR) analysis was run on the Thermo Fisher QuantStudio 3 system. Primers were designed *de novo* spanning exon-exon junctions using the Primer Blast design tool (NCBI) and are included in Supplementary Table 1. Published primer sequences for the housekeeping gene *ODC* (*odc1*, encoding ornithine decarboxylase) were used for reference measurement (Agius et al., 2000). Raw quantification cycle values (Cq/

Ct, using the 'Baseline Threshold' setting) were normalised to the *ODC* reference and exponentiated to obtain $2^{-\Delta Ct}$ values used for fold change quantification.

For immunohistochemistry, samples are fixed in 4 % paraformaldehyde in PBS (P6148, Sigma) for 1 h at room temperature or overnight at 4 °C and washed in PBS containing 0.1 % Tween-20 (P1379, Sigma). To bleach pigment found in blastula cells, 1 h of 3 % hydrogen peroxide solution was used. Samples were permeabilised in 0.1–0.2 % Triton X-100 (T8787, Sigma) in PBS and blocked in 10 % NGS (Normal Goat Serum, PCN5000, Thermo Fisher) for at least 1 h. Both primary antibodies for β-catenin (C2206, Sigma, 1 in 300) and secondary antibodies AlexaFluor-555 (A21428, Invitrogen) or AlexaFluor-488 (A21206, Invitrogen) were diluted in NGS and incubated for at least 4 h. After final PBS-Tween washes, samples were dehydrated in methanol and cleared for imaging using a mixture of benzyl alcohol and benzyl benzoate (1 to 2 ratio). DAPI (D1306, Sigma, 1 in 1000) was used for the detection of nuclei.

4.4. Image acquisition and analysis

An inverted Zeiss widefield microscope (Zeiss Axiovert 200 M, Hamamatsu Orca-ER camera) was used to visualise the extent of mechanical compression in AC explant experiments. Fluorescent imaging was performed on an inverted Zeiss LSM 980 microscope with Airyscan 2 in multiplexing mode or an upright laser scanning confocal microscope (SP8, Leica Microsystems). Image analysis was performed using FIJI (Schindelin et al., 2012) and Python's scikit-image library (van der Walt et al., 2014). Segmentation was done using an interactive machine learning-based pixel classification tool 'ilastik' (https://www.ilastik.org/) (Berg et al., 2019) and StarDist specifically for nuclear 2D shape segmentation (Schmidt et al., 2018). Fluorescence intensity was measured using the mean pixel value in FIJI.

4.5. Statistical analysis

For comparisons between two independent normally distributed groups an unpaired Welch *t*-test was used. Analysis of variance (one-way ANOVA) was used for multiple comparisons between more than two distributions followed by a Tukey's Honest Significant Difference post-hoc test to obtain *p*-values. Cohen's d test was used to calculate effect size (Lakens, 2013). Kolmogorov-Smirnov and Shapiro-Wilk's (for sample size under 50) normality tests combined with visual inspection of a quantile-quantile plot were used to determine whether data follow a normal distribution. Where normality could not be assumed, a non-parametric one-sided Mann-Whitney U rank sum test was used when the data showed a clear trend, otherwise a two-sided test was used. Kruskal-Wallis rank sum test was used to confirm the significance of multiple comparisons. In Fig. 7D–E two values were removed as outliers (Grubb's test, $p < 0.0001$) without affecting statistical significance of difference between means. Statistical tests were performed using the following R packages: 'stats', 'rstatix' and 'ggpubr'. Redpoint and error bars represent the median value with 95 % confidence intervals unless stated otherwise. *P*-values from all statistical tests are represented with asterisks n.s. $= p > 0.05$, * $= p < 0.05$, ** $= p < 0.01$, *** $= p < 0.001$, **** $= p < 0.0001$.

Supplementary data to this article can be found online at https://doi.org/10.1016/j.cdev.2024.203984.

CRediT authorship contribution statement

Matyas Bubna-Litic: Writing – review & editing, Writing – original draft, Methodology, Investigation, Formal analysis, Conceptualization. **Guillaume Charras:** Writing – review & editing. **Roberto Mayor:** Writing – review & editing, Writing – original draft, Supervision, Project administration, Funding acquisition, Conceptualization.

Funding

Work in R.M.'s laboratory is supported by grants from the Medical Research Council (MR/S007792/1), Biotechnology and Biological Sciences Research Council (M008517, BB/T013044) and Wellcome Trust (102489/Z/13/Z). M.B-L. was supported by the UK Biotechnology and Biological Sciences Research Council (BBSRC) through the London Interdisciplinary Biosciences Consortium.

Declaration of competing interest

None.

Acknowledgements

We thank Alexandre Kabla for kindly loaning the compression apparatus, Edward De Robertis and Caroline Hill for plasmids. We further thank Jonas Hartmann and Lucas Alvizi who provided feedback and assisted with data analysis.

References

Agathon, A., Thisse, C., Thisse, B., Jul. 2003. The molecular nature of the zebrafish tail organizer. Nature 424 (6947), 448–452. https://doi.org/10.1038/nature01822.

Agius, E., Oelgeschläger, M., Wessely, O., Kemp, C., De Robertis, E.M., Mar. 2000. Endodermal nodal-related signals and mesoderm induction in Xenopus. Development 127 (6), 1173–1183.

Ariizumi, T., Sawamura, K., Uchiyama, H., Asashima, M., Dec. 1991. Dose and time-dependent mesoderm induction and outgrowth formation by activin A in Xenopus laevis. Int. J. Dev. Biol. 35 (4), 407–414.

Ariizumi, T., Takano, K., Ninomiya, H., Asashima, M., Dec. 1998. Activin-treated urodele animal caps: I. Mesoderm and endoderm differentiation of salamander animal caps. jzoo 15 (6), 887–892. https://doi.org/10.2108/zsj.15.887.

Alasaadi, D., Alvizi, L., Hartmann, J., Stillman, N., Moghe, P., Hiiragi, T., Mayor, R., 2024. Competence for neural crest induction is controlled by hydrostatic pressure through Yap. Nat. Cell. Biol. 25, 530–541.

Ariizumi, T., Michiue, T., Asashima, M., Jan. 2017. In vitro induction of Xenopus embryonic organs using animal cap cells. Cold Spring Harb. Protoc. 2017 (12). https://doi.org/10.1101/pdb.prot097410 p. pdb. prot 097410.

Bauer, D.V., Huang, S., Moody, S.A., May 1994. The cleavage stage origin of Spemann's organizer: analysis of the movements of blastomere clones before and during gastrulation in Xenopus. Development 120 (5), 1179–1189. https://doi.org/10.1242/dev.120.5.1179.

Benham-Pyle, B.W., Pruitt, B.L., Nelson, W.J., May 2015. Mechanical strain induces E-cadherin–dependent Yap1 and β-catenin activation to drive cell cycle entry. Science 348 (6238), 1024–1027. https://doi.org/10.1126/science.aaa4559.

Berg, S., et al., Dec. 2019. ilastik: interactive machine learning for (bio)image analysis. Nat. Methods 16 (12), 12. https://doi.org/10.1038/s41592-019-0582-9.

Briggs, J.A., et al., Jun. 2018. The dynamics of gene expression in vertebrate embryogenesis at single-cell resolution. Science 360 (6392), eaar5780. https://doi.org/10.1126/science.aar5780.

Bright, A.R., et al., May 2021. Combinatorial transcription factor activities on open chromatin induce embryonic heterogeneity in vertebrates. EMBO J. 40 (9), e104913. https://doi.org/10.15252/embj.2020104913.

Bruce, A.E.E., Winklbauer, R., Sep. 2020. Brachyury in the gastrula of basal vertebrates. Mech. Dev. 163, 103625. https://doi.org/10.1016/j.mod.2020.103625.

Brunet, T., et al., 2013. Evolutionary conservation of early mesoderm specification by mechanotransduction in Bilateria. Nat. Commun. 4, 2821. https://doi.org/10.1038/ncomms3821.

Chien, Y.-H., Keller, R., Kintner, C., Shook, D.R., Nov. 2015. Mechanical strain determines the axis of planar polarity in ciliated epithelia. Curr. Biol. 25 (21), 2774–2784. https://doi.org/10.1016/j.cub.2015.09.015.

Collinet, C., Lecuit, T., Apr. 2021. Programmed and self-organized flow of information during morphogenesis. Nat. Rev. Mol. Cell Biol. 22 (4), 245–265. https://doi.org/10.1038/s41580-020-00318-6.

Cornell, R.A., Kimelman, D., Feb. 1994. Activin-mediated mesoderm induction requires FGF. Development 120 (2), 453–462. https://doi.org/10.1242/dev.120.2.453.

Crease, D.J., Dyson, S., Gurdon, J.B., Apr. 1998. Cooperation between the activin and Wnt pathways in the spatial control of organizer gene expression. Proc. Natl. Acad. Sci. U. S. A. 95 (8), 4398–4403. https://doi.org/10.1073/pnas.95.8.4398.

Dale, L., Nov. 1997. Development: morphogen gradients and mesodermal patterning. Curr. Biol. 7 (11), R698–R700. https://doi.org/10.1016/S0960-9822(06)00359-9.

Dale, L., Slack, J.M., Jun. 1987. Regional specification within the mesoderm of early embryos of Xenopus laevis. Development 100 (2), 279–295. https://doi.org/10.1242/dev.100.2.279.

De Belly, H., Paluch, E.K., Chalut, K.J., Jul. 2022. Interplay between mechanics and signalling in regulating cell fate. Nat. Rev. Mol. Cell Biol. 23 (7), 7. https://doi.org/10.1038/s41580-022-00472-z.

Deng, F., et al., Feb. 2018. YAP triggers the Wnt/β-catenin signalling pathway and promotes enterocyte self-renewal, regeneration and tumorigenesis after DSS-induced injury. Cell Death Dis. 9 (2), 2. https://doi.org/10.1038/s41419-017-0244-8.

Ding, Y., et al., Apr. 2017. Spemann organizer transcriptome induction by early beta-catenin, Wnt, Nodal, and Siamois signals in Xenopus laevis. Proc. Natl. Acad. Sci. 114 (15), E3081–E3090. https://doi.org/10.1073/pnas.1700766114.

Dingwell, K.S., Smith, J.C., Oct. 2018. Dissecting and culturing animal cap explants. Cold Spring Harb. Protoc. 2018 (10). https://doi.org/10.1101/pdb.prot097329.

Dyer, C., Blanc, E., Stanley, R.J., Knight, R.D., Jan. 2015. Dissecting the role of Wnt signaling and its interactions with FGF signaling during midbrain neurogenesis. Neurogenesis 2 (1), e1057313. https://doi.org/10.1080/23262133.2015.1057313.

Elosegui-Artola, A., et al., Nov. 2017. Force triggers YAP nuclear entry by regulating transport across nuclear pores. Cell 171 (6), 1397–1410 e14. https://doi.org/10.1016/j.cell.2017.10.008.

Emig, A.A., Williams, M.L.K., May 2023. Gastrulation morphogenesis in synthetic systems. Semin. Cell Dev. Biol. 141, 3–13. https://doi.org/10.1016/j.semcdb.2022.07.002.

Fagotto, F., Funayama, N., Gluck, U., Gumbiner, B.M., Mar. 1996. Binding to cadherins antagonizes the signaling activity of beta-catenin during axis formation in Xenopus. J. Cell Biol. 132 (6), 1105–1114. https://doi.org/10.1083/jcb.132.6.1105.

Gayrard, C., Bernaudin, C., Déjardin, T., Seiler, C., Borghi, N., Jan. 2018. Src- and confinement-dependent FAK activation causes E-cadherin relaxation and β-catenin activity. J. Cell Biol. 217 (3), 1063–1077. https://doi.org/10.1083/jcb.201706013.

Green, J., 1999. The animal cap assay. Methods Mol. Biol. 127, 1–13. https://doi.org/10.1385/1-59259-678-9:1.

Green, J.B.A., Smith, J.C., Sep. 1990. Graded changes in dose of a Xenopus activin A homologue elicit stepwise transitions in embryonic cell fate. Nature 347 (6291), 6291. https://doi.org/10.1038/347391a0.

Green, J.B.A., Cook, T.L., Smith, J.C., Grainger, R.M., Aug. 1997. Anteroposterior neural tissue specification by activin-induced mesoderm. Proc. Natl. Acad. Sci. 94 (16), 8596–8601. https://doi.org/10.1073/pnas.94.16.8596.

Green, J.B.A., Dominguez, I., Davidson, L.A., 2004. Self-organization of vertebrate mesoderm based on simple boundary conditions. Dev. Dyn. 231 (3), 576–581. https://doi.org/10.1002/dvdy.20163.

Guger, K.A., Gumbiner, B.M., Nov. 1995. beta-Catenin has Wnt-like activity and mimics the Nieuwkoop signaling center in Xenopus dorsal-ventral patterning. Dev. Biol. 172 (1), 115–125. https://doi.org/10.1006/dbio.1995.0009.

Gurdon, J.B., Bourillot, P.-Y., Oct. 2001. Morphogen gradient interpretation. Nature 413 (6858), 6858. https://doi.org/10.1038/35101500.

Gurdon, J.B., Kato, K., Lemaire, P., Jan. 1993. The community effect, dorsalization and mesoderm induction. Curr. Opin. Genet. Dev. 3 (4), 662–667. https://doi.org/10.1016/0959-437X(93)90104-W.

Hikasa, H., Sokol, S.Y., Jan. 2013. Wnt signaling in vertebrate axis specification. Cold Spring Harb. Perspect. Biol. 5 (1), a007955. https://doi.org/10.1101/cshperspect.a007955.

Holtfreter, J., 1943. A study of the mechanics of gastrulation. Part I. J. Exp. Zool. 94 (3), 261–318. https://doi.org/10.1002/jez.1400940302.

Huang, Y.-L., Niehrs, C., Apr. 2014. Polarized Wnt signaling regulates ectodermal cell fate in Xenopus. Dev. Cell 29 (2), 250–257. https://doi.org/10.1016/j.devcel.2014.03.015.

Ishibashi, H., Matsumura, N., Hanafusa, H., Matsumoto, K., De Robertis, E.M., Kuroda, H., 2008. Expression of siamois and twin in the blastula chordin/noggin signaling center is required for brain formation in Xenopus laevis embryos. Mech. Dev. 125 (1–2), 58–66. https://doi.org/10.1016/j.mod.2007.10.005.

Itoh, K., Sokol, S.Y., Sep. 1999. Axis determination by inhibition of Wnt signaling in Xenopus. Genes Dev. 13 (17), 2328–2336.

Joubin, K., Stern, C.D., Sep. 1999. Molecular interactions continuously define the organizer during the cell movements of gastrulation. Cell 98 (5), 559–571. https://doi.org/10.1016/S0092-8674(00)80044-6.

Joubin, K., Stern, C.D., 2001. Formation and maintenance of the organizer among the vertebrates. Int. J. Dev. Biol. 45 (1), 165–175.

Kaneda, T., Motoki, J.D., Sep. 2012. Gastrulation and pre-gastrulation morphogenesis, inductions, and gene expression: similarities and dissimilarities between urodelean and anuran embryos. Dev. Biol. 369 (1), 1–18. https://doi.org/10.1016/j.ydbio.2012.05.019.

Kiecker, C., Niehrs, C., Nov. 2001. A morphogen gradient of Wnt/beta-catenin signalling regulates anteroposterior neural patterning in Xenopus. Development 128 (21), 4189–4201. https://doi.org/10.1242/dev.128.21.4189.

Kiecker, C., Bates, T., Bell, E., 2016. Molecular specification of germ layers in vertebrate embryos. Cell. Mol. Life Sci. 73, 923–947. https://doi.org/10.1007/s00018-015-2092-y.

Knoetgen, H., Teichmann, U., Wittler, L., Viebahn, C., Kessel, M., Sep. 2000. Anterior neural induction by nodes from rabbits and mice. Dev. Biol. 225 (2), 370–380. https://doi.org/10.1006/dbio.2000.9834.

Kuroda, H., Wessely, O., Robertis, E.M.D., May 2004. Neural induction in Xenopus: requirement for ectodermal and endomesodermal signals via chordin, noggin, β-catenin, and cerberus. PLoS Biol 2 (5), e92. https://doi.org/10.1371/journal.pbio.0020092.

Lakens, D., Nov. 2013. Calculating and reporting effect sizes to facilitate cumulative science: a practical primer for t-tests and ANOVAs. Front. Psychol. 4, 863. https://doi.org/10.3389/fpsyg.2013.00863.

Logan, M., Mohun, T., Jul. 1993. Induction of cardiac muscle differentiation in isolated animal pole explants of Xenopus laevis embryos. Development 118 (3), 865–875. https://doi.org/10.1242/dev.118.3.865.

Miller, C.J., Davidson, L.A., Oct. 2013. The interplay between cell signalling and mechanics in developmental processes. Nat. Rev. Genet. 14 (10), 10. https://doi.org/10.1038/nrg3513.

Moris, N., Martinez Arias, A., Steventon, B., Oct. 2020. Experimental embryology of gastrulation: pluripotent stem cells as a new model system. Curr. Opin. Genet. Dev. 64, 78–83. https://doi.org/10.1016/j.gde.2020.05.031.

Muncie, J.M., Ayad, N.M.E., Lakins, J.N., Xue, X., Fu, J., Weaver, V.M., Dec. 2020. Mechanical tension promotes formation of gastrulation-like nodes and patterns mesoderm specification in human embryonic stem cells. Dev. Cell 55 (6), 679–694. e11. https://doi.org/10.1016/j.devcel.2020.10.015.

Niehrs, C., Jun. 2004. Regionally specific induction by the Spemann–Mangold organizer. Nat. Rev. Genet. 5 (6), 6. https://doi.org/10.1038/nrg1347.

Nieuwkoop, P.D., Faber, J., Gerhart, J., Kirschner, M. (Eds.), 1994. Normal Table of *Xenopus laevis* (Daudin): A Systematical and Chronological Survey of the Development from the Fertilized Egg Till the End of Metamorphosis. Garland Science, New York. https://doi.org/10.1201/9781003064565.

Ninomiya, H., Elinson, R.P., Winklbauer, R., Jul. 2004. Antero-posterior tissue polarity links mesoderm convergent extension to axial patterning. Nature 430 (6997), 6997. https://doi.org/10.1038/nature02620.

Papan, C., Boulat, B., Velan, S.S., Fraser, S.E., Jacobs, R.E., 2007. Formation of the dorsal marginal zone in Xenopus laevis analyzed by time-lapse microscopic magnetic resonance imaging. Dev. Biol. 305 (1), 161–171. https://doi.org/10.1016/j.ydbio.2007.02.005.

Pearl, E., Morrow, S., Noble, A., Lerebours, A., Horb, M., Guille, M., Apr. 2017. An optimized method for cryogenic storage of Xenopus sperm to maximise the effectiveness of research using genetically altered frogs. Theriogenology 92, 149–155. https://doi.org/10.1016/j.theriogenology.2017.01.007.

Piccolo, S., Sladitschek-Martens, H.L., Cordenonsi, M., Aug. 2022. Mechanosignaling in vertebrate development. Dev. Biol. 488, 54–67. https://doi.org/10.1016/j.ydbio.2022.05.005.

Pukhlyakova, E., Aman, A.J., Elsayad, K., Technau, U., Jun. 2018. β-Catenin–dependent mechanotransduction dates back to the common ancestor of Cnidaria and Bilateria. Proc. Natl. Acad. Sci. 115 (24), 6231–6236. https://doi.org/10.1073/pnas.1713682115.

Reddy, P.C., Gungi, A., Ubhe, S., Pradhan, S.J., Kolte, A., Galande, S., Nov. 2019. Molecular signature of an ancient organizer regulated by Wnt/β-catenin signalling during primary body axis patterning in Hydra. Commun Biol 2 (1), 1–11. https://doi.org/10.1038/s42003-019-0680-3.

Röper, J.-C., et al., Jul. 2018. The major β-catenin/E-cadherin junctional binding site is a primary molecular mechano-transductor of differentiation in vivo. eLife 7, e33381. https://doi.org/10.7554/eLife.33381.

Saadaoui, M., Rocancourt, D., Roussel, J., Corson, F., Gros, J., Jan. 2020. A tensile ring drives tissue flows to shape the gastrulating amniote embryo. Science 367 (6476), 453–458. https://doi.org/10.1126/science.aaw1965.

Sander, V., Reversade, B., De Robertis, E.M., Jun. 2007. The opposing homeobox genes Goosecoid and Vent1/2 self-regulate Xenopus patterning. EMBO J. 26 (12), 2955–2965. https://doi.org/10.1038/sj.emboj.7601705.

Satou-Kobayashi, Y., Kim, J.-D., Fukamizu, A., Asashima, M., Jul. 2021. Temporal transcriptomic profiling reveals dynamic changes in gene expression of Xenopus animal cap upon activin treatment. Sci. Rep. 11 (1), 14537. https://doi.org/10.1038/s41598-021-93524-x.

Schindelin, J., et al., Jul. 2012. Fiji: an open-source platform for biological-image analysis. Nat. Methods 9 (7), 7. https://doi.org/10.1038/nmeth.2019.

Schmidt, U., Weigert, M., Broaddus, C., Myers, G., 2018. Cell Detection With Star-convex Polygons, 11071, pp. 265–273. https://doi.org/10.1007/978-3-030-00934-2_30.

Schohl, A., Fagotto, F., Jan. 2002. β-Catenin, MAPK and Smad signaling during early Xenopus development. Development 129 (1), 37–52. https://doi.org/10.1242/dev.129.1.37.

Schohl, A., Fagotto, F., Jul. 2003. A role for maternal β-catenin in early mesoderm induction in Xenopus. EMBO J. 22 (13), 3303–3313. https://doi.org/10.1093/emboj/cdg328.

Shellard, A., Szabó, A., Trepat, X., Mayor, R., Oct. 2018. Supracellular contraction at the rear of neural crest cell groups drives collective chemotaxis. Science 362 (6412), 339–343. https://doi.org/10.1126/science.aau3301.

Shook, D.R., Kasprowicz, E.M., Davidson, L.A., Keller, R., Mar. 2018. Large, long range tensile forces drive convergence during Xenopus blastopore closure and body axis elongation. eLife 7, e26944. https://doi.org/10.7554/eLife.26944.

Sive, H.L., Grainger, R.M., Harland, R.M., 2000. Early Development of *Xenopus Laevis*: A Laboratory Manual. CSHL Press.

Skory, R.M., et al., May 2023. The nuclear lamina couples mechanical forces to cell fate in the preimplantation embryo via actin organization. Nat. Commun. 14 (1), 3101. https://doi.org/10.1038/s41467-023-38770-5.

Spemann, H., Mangold, H., 1924. Ueber Induktion von Embryoalanlagen dürch Implantation artfremder Organisatoren. W. Roux' Arch. 100, 599–638.

Srivastava, N., Kay, R.R., Kabla, A.J., Mar. 2017. Method to study cell migration under uniaxial compression. Mol. Biol. Cell 28 (6), 809–816. https://doi.org/10.1091/mbc.E16-08-0575.

Theveneau, E., et al., Jul. 2010. Collective chemotaxis requires contact-dependent cell polarity. Dev. Cell 19 (1), 39–53. https://doi.org/10.1016/j.devcel.2010.06.012.

Ulmer, B., et al., Feb. 2017. A novel role of the organizer gene Goosecoid as an inhibitor of Wnt/PCP-mediated convergent extension in Xenopus and mouse. Sci. Rep. 7 (1), 1. https://doi.org/10.1038/srep43010.

Uochi, T., Asashima, M., Dec. 1996. Sequential gene expression during pronephric tubule formation in vitro in Xenopus ectoderm. Dev. Growth Differ. 38 (6), 625–634. https://doi.org/10.1046/j.1440-169X.1996.t01-5-00006.x.

van der Walt, S., et al., 2014. scikit-image: image processing in Python. PeerJ 2, e453. https://doi.org/10.7717/peerj.453.

Vianello, S., Lutolf, M.P., Mar. 2019. Understanding the mechanobiology of early mammalian development through bioengineered models. Dev. Cell 48 (6), 751–763. https://doi.org/10.1016/j.devcel.2019.02.024.

Wen, J.W., Winklbauer, R., Aug. 2017. Ingression-type cell migration drives vegetal endoderm internalisation in the Xenopus gastrula. eLife 6, e27190. https://doi.org/10.7554/eLife.27190.

Winklbauer, R., Parent, S.E., Apr. 2017. Forces driving cell sorting in the amphibian embryo. Mech. Dev. 144, 81–91. https://doi.org/10.1016/j.mod.2016.09.003.